Received January 18, 2021, accepted February 1, 2021, date of publication February 8, 2021, date of current version February 24, 2021.

Digital Object Identifier 10.1109/ACCESS.2021.3057941

Design and Implementation of UWB Slot-Loaded Printed Antenna for Microwave and Millimeter Wave Applications

SARA YEHIA ABDEL FATAH[1], EHAB K. I. HAMAD[2], WAEL SWELAM[3], A. M. M. A. ALLAM[4], MOHAMED FATHY ABO SREE[3], AND HESHAM A. MOHAMED[5], (Member, IEEE)

[1]Department of Mechatronics Engineering and Automation, Faculty of Engineering, Egyptian Chinese University, Cairo, Egypt
[2]Department of Electrical Engineering, Faculty of Engineering, Aswan University, Aswan, Egypt
[3]Department of Electronics and Communications Engineering, Arab Academy for Science, Technology and Maritime Transport, Cairo, Egypt
[4]Head of Information Technology in GUC, Cairo, Egypt
[5]Department of Microstrip Electronics Research Institute (ERI), Giza 12622, Egypt

Corresponding author: Sara Yehia Abdel Fatah (phd-ecu-s@hotmail.com)

ABSTRACT In this paper, single-layer ultra-Wide Band (UWB) microstrip patch antennas loaded with asymmetrical U-shaped slot in both microwave and millimeter wave applications are presented. These novel antennas cover a fractional bandwidth around 40% in both microwave and millimeter applications. The applications cover the C-band (4-8) GHz, V-band (40-75) GHz, and W-band (75-110) GHz. In addition to that, it is the sole article that cover the bands (5.15-5.825) GHz and (8.025-8.4) GHZ for WiMaX and ITU band applications, respectively. Moreover, it covers three bands for Automotive radar applications within (71-76) GHz, (81-86) GHz, and (92-95) GHz, in addition to further 5G/mm-wave applications at 60 GHz. Each antenna is coaxial fed and implemented on a Roger 5880 substrate with relative dielectric constant of 2.2, thickness of 1.575 *mm* and loss tangent of 0.0009. They operate over the frequency band (5.5-9.5) GHz for microwave band and (55-95) GHz for mm-wave band. To achieve either a notch in other bands or develop a multi-band structure, the conventional ground is replaced by two different structures. The first ground is an array of patches and the other is a mushroom ground. The first ground results in a notch within the band (73-79) GHz while the second one achieves a multi-band within (55-68) GHz and (81-95) GHz. Both antennas are simulated and verified using Finite Difference Time-Domain analysis (FDTD); CST Microwave Studio and Finite Element Method (FEM); Ansoft HFSS. For microwave band, the antenna is fabricated and measured for verification. Concerning the mm-wave version, three different types of ground planes are presented; traditional, periodic structure of patches and mushroom. The structure with periodic patches conducts the same band as the traditional ground plane does. This is a prestep for the design of the notches. The mushroom ground is carried out for multi-band applications. The average gain of the antennas is 7 dB.The measured two dimensional cuts of the radiation pattern, radiation efficiency, and reflection coefficient of the microwave version are presented and are in good agreement with the simulated results while for the mm-wave antenna the same parameters are simulated with two different methods and are in good agreement.

INDEX TERMS U-Slotted patch antenna, millimeter wave, microwave band, mushroom ground antennas, metamaterial.

I. INTRODUCTION

Along with the great increase in the mobile data requirements, despite that the microwave spectrum has a great application in mobile and wireless communications systems, the fifth generation mobile network (5G) is expected to make use of a large quota of the mm-wave spectrum bands [1]–[4], which is expected to significantly increase the current communication capacity.

Prior to optimization, the initial dimensions of the antenna in the mircrowave band were PL = 12.5 *mm* and PW = 15.8 *mm*. On the other hand, for the mm-wave band, the initial dimensions were PL = 0.26 *mm* and PW = 1.58 *mm*.

These antennas can be used for different airborne applications, point-to-point communication systems, Synthetic Aperture Radar (SAR) applications [5] and cellular systems.

The associate editor coordinating the review of this manuscript and approving it for publication was Wenjie Feng.

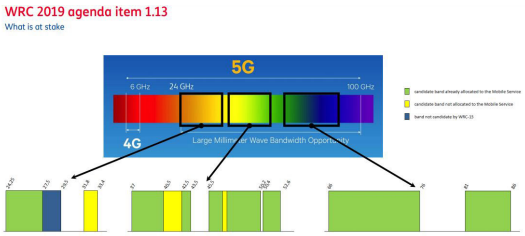

FIGURE 1. 5G Spectrum in Microwave and mm-wave bandwidths - ITU Standardization-July 2019.

Moreover, people's needs and way of living change, and the demand to improve communication system facilities increases. Most of the devices were developed and reached much higher standards in order to have low profile, light weight, and low cost which are often highly demanded. To achieve these requirements microstrip patch antenna has been widely used because of its compact structure, low profile, and easy integration [6]. However, conventional microstrip antennas suffer from very narrow frequency band, which is typically only a fraction of a percent or at the most few percent [1]. On the other hand, core differences currently exist between the ongoing communication systems particularly in terms of directivity, propagation losses and antenna technology [7]–[13].

In order to support the 5G for both the small quota of the microwave band and the large quota of the mm-wave band, several methods have been presented to enhance the bandwidth of microstrip patch antennas [14], [15]. One of the most popular ways is to introduce some slots into the patch radiators [16], which can yield extra controllable resonances for bandwidth enhancement. Another approach used recently by researchers [12], [17]–[22] is to insert shorting vias into the dielectric substrate, resulting in the expansion of the impedance bandwidths of the antennas.

The goal of this work is to develop a low-profile wide-band antenna with acceptable radiation performance covering both the frequency bands (5.5-9.5) GHz and (55-95) GHz for 5G and mm-wave applications. The antenna is designed, analyzed, fabricated, and measured using ROHDE & SCHWARZ ZVB20 vector Network Analyzer and anechoic chamber for microwave band. Due to limitation in fabrication resources in mm-wave, the antenna in this band is simulated using both FDTD; CST Microwave Studio and FEM; Ansoft HFSS for the validation of the presented work. On the other hand, for mm-wave band antenna structure a ground layer of an array of patches and a mushroom ground-type structure [23] are added to the antenna to notch some bands and achieves multi-band antenna. The paper is organized as follows. The designs for both antennas are outlined in Section II. In Section III, simulation and measured results are presented. Finally, conclusions are drawn in Section IV.

II. ANTENNA DESIGN

This section is devoted to the antenna design in both microwave and mm-wave bands operating from 5.5 GHz to 9.5 GHz and 55 GHz to 95 GHz respectively. It is based on the equations of length and width of printed patch antenna [1]. Thus, the preliminary values of the antenna length PL and width PW can be determined from these equations and later optimized.

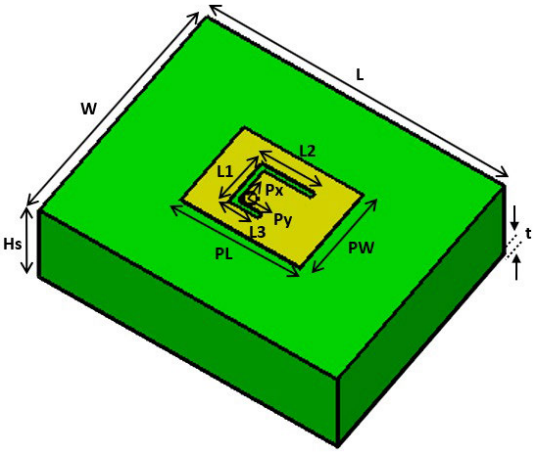

FIGURE 2. The proposed antenna for both bands.

TABLE 1. Antenna dimensions of the proposed antenna.

Parameter	Microwave band (mm)	mm-wave band (mm)
L	50	5
W	40	4
t	0.015	0.015
hs	1.575	1.575
L1	18	1.8
L2	12	1.2
L3	5	0.5
Px	1.9	0.19
Py	2.3	0.23
PL	20	2
PW	15	1.5

$$W = \frac{c_0}{2f_r}\sqrt{\frac{2}{\epsilon_r + 1}} \tag{1}$$

$$L = \frac{c_0}{2f_r\sqrt{\epsilon_{reff}}} - 2\Delta L \tag{2}$$

$$\Delta L = 0.412h\frac{(\epsilon_{reff} + 0.3)(\frac{W}{h} + 0.264)}{(\epsilon_{reff} - 0.258)(\frac{W}{h} + 0.8)} \tag{3}$$

$$\epsilon_{reff} = \frac{\epsilon_r + 1}{2} + \frac{\epsilon_r - 1}{2}[1 + 12\frac{h}{W}]^{-0.5}, \quad \frac{W}{h} > 1 \tag{4}$$

Figure 2 illustrates the proposed antenna structure with its dimension are depicted in table1. The patch is implemented on a Roger 5880 RT substrate with relative dielectric constant 2.2 and loss tangent 0.0009. The patch is loaded with a slot and fed using coaxial probe. The overall dimensions of the antenna are $4 \times 5 \times 1.575\ mm^3$ for mm-band and $40 \times 50 \times 1.575\ mm^3$ for microwave band.

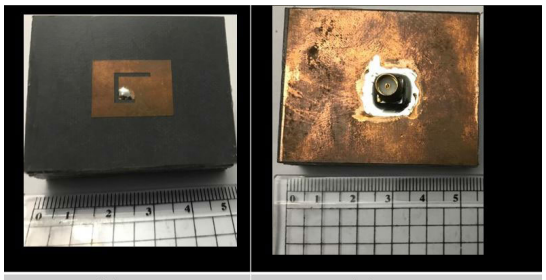

FIGURE 3. Fabrication of proposed antenna (a) Top layer (b) Bottom layer.

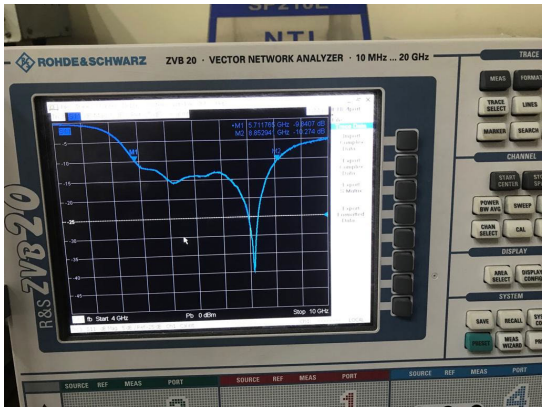

FIGURE 4. Measurement of reflection coefficient (S_{11}).

III. SIMULATED AND MEASURED RESULTS

A. ANTENNA OPERATING IN MICROWAVE BAND (5.5-9.5) GHz

The antenna is fabricated as shown in figure 3 and measured using ROHDE & SCHWARZ ZVB20 vector Network Analyzer and anechoic chamber as depicted in figure 4 and figure 5. A parametric sweep of the feed position (x-position, y-position) is carried out to study its effect on the reflection coefficient. Figure 6 shows that reflection coefficient for different x positions and y positions. It is clear that the value at x = 1.9 *mm* left from the center and y = 2.3 *mm* down from the center is the optimum location.

Figure 7 illustrates the simulated and measured reflection coefficients. The measurements are carried out using two different network analyzers. It is clear that the antenna operates in the band from 5.5 GHz to 9.5 GHz. The measured and simulated realized gain of the antenna is presented in figure 8. It is bounded between 4 and 9 dB. Since the physical dimensions of the antenna is maintained unaltered, the higher the frequency, the lower the wavelength, the higher the electrical dimensions of the antenna structure, hence the gain increases [24], [25].

The two-dimensional radiation pattern at two different frequencies 5.6 GHz and 7.8 GHz in the two principle planes ($\Phi = 0°$ & $\Phi = 90°$) are depicted in figures 9. Figures 10 and 11 show the Co and X-polarization, and the axial ratio over the operating band respectively. It is noticed

FIGURE 5. Measurement of the radiation pattern and gain in anechoic chamber.

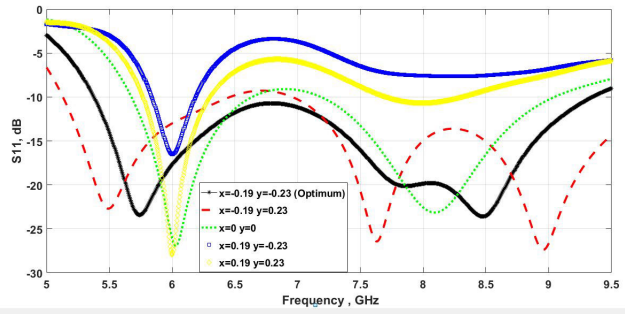

FIGURE 6. Reflection coefficient of different feed positions.

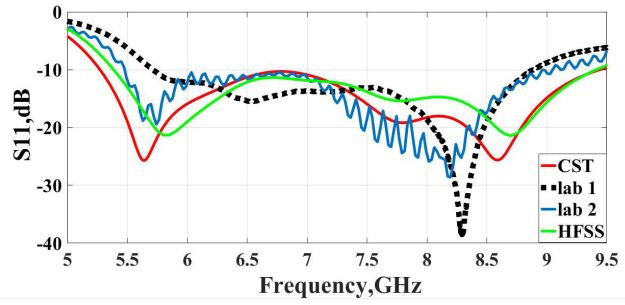

FIGURE 7. Simulated and measured reflection coefficient.

that the antenna is linearly polarized and the axial ratio is over 3dB over the whole band. [26] Notice the a fair agreement between the measured and simulated patterns. Radiation efficiency is illustrated in figure 12 where the measured and simulated results match. The zoomed in radiation efficiency

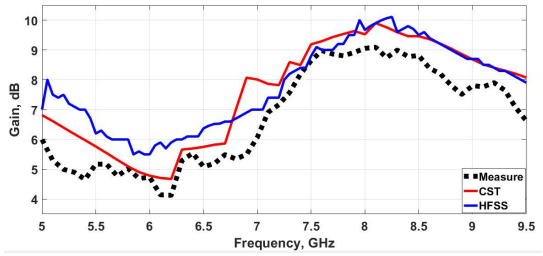

FIGURE 8. Simulated and measured realized gain.

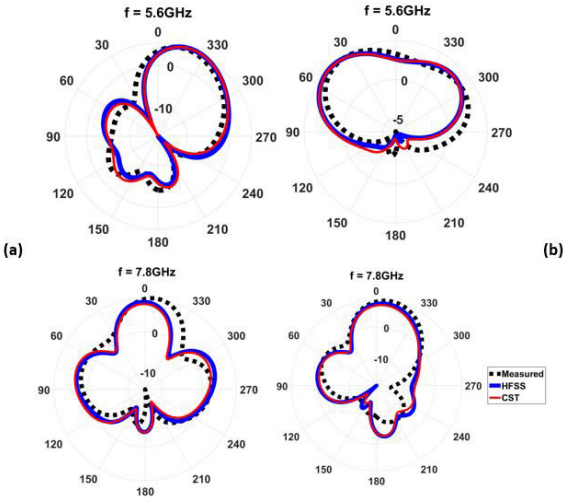

FIGURE 9. Simulated and measured 2D radiation patterns (a) E-plane $\Phi = 0°$, (b) H-plane $\Phi = 90°$.

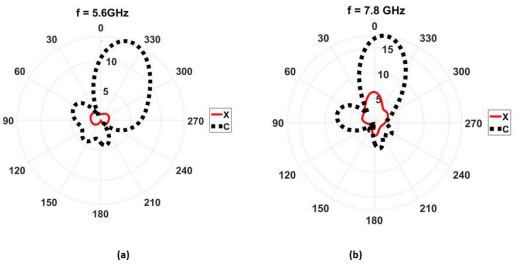

FIGURE 10. Co and X-polarization for frequencies 5.6 GHz and 7.8 GHz.

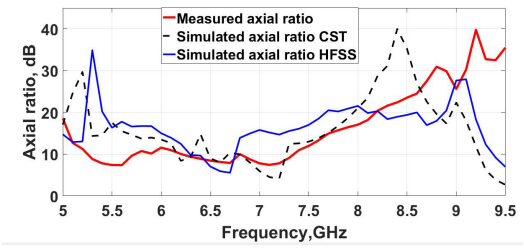

FIGURE 11. Simulated and measured axial ratio.

for the range (5.5-9.5) GHz clearly show that it is not flat, as it fluctuates between 0.92 and 0.985. The total efficiency has the same behavior as the realized gain but the radiation

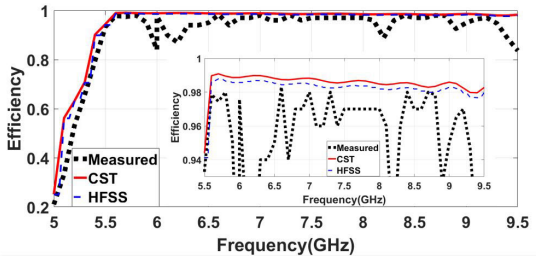

FIGURE 12. Simulated and measured radiation efficiency.

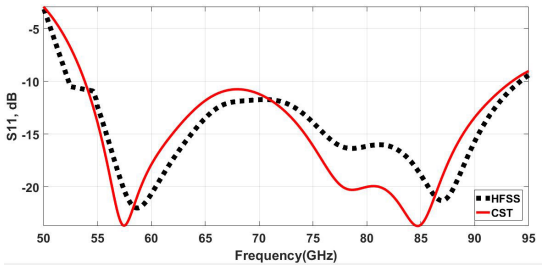

FIGURE 13. Comparison of the simulated reflection coefficient using HFSS and CST.

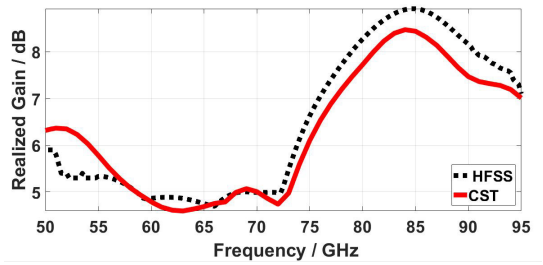

FIGURE 14. Comparison of the simulated realized gain using HFSS and CST.

efficiency generated by CST and HFSS shows nearly perfect behavior. The antenna has an outstanding radiation efficiency that exceeds 95% and thus, has a flat-like response across the whole band [27], [28].

B. ANTENNA OPERATING IN MILLIMETER BAND [55 TO 95 GHz]

The reflection coefficient of the antenna operating in the mm-wave band is determined using FDTD and FEM methods. The simulated results are illustrated in figure 13. The antenna operates over the frequency band 55 GHz to 95 GHz. There is a fair agreement between the simulated results using both tools. Similarly, a simulation of both the realized gain and radiation efficiency are carried out and illustrated in figures 14 and 15 respectively. Notice the good agreement between the results. Again, the zoomed in radiation efficiency for the range (55-95) GHz clearly show that it is not flat, as it fluctuates between 0.92 and 0.985.

Further more the two-dimensional radiation patterns extracted from both simulators are accurately coincident as

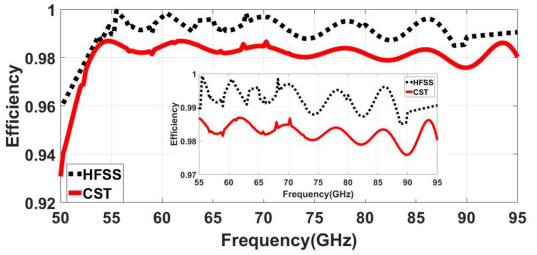

FIGURE 15. Comparison of radiation efficiency using HFSS and CST.

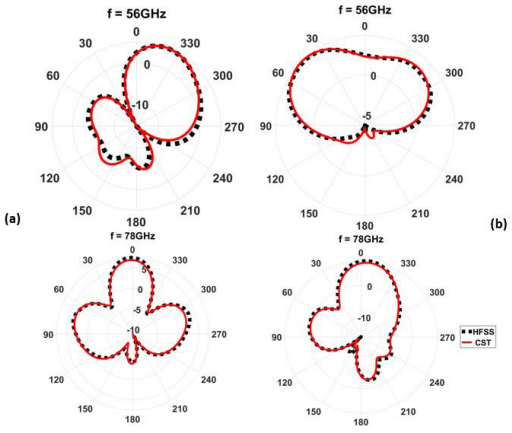

FIGURE 16. Comparison of 2D radiation patterns using HFSS and CST (a) E-plane $\Phi = 0°$ (b) H-plane $\Phi = 90°$.

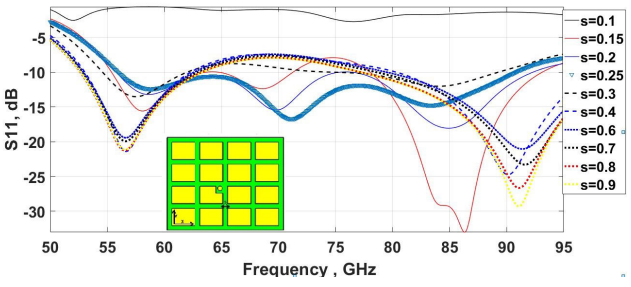

FIGURE 17. Reflection coefficients with different separations.

shown in figure 16. To achieve an ultra-wide band, the traditional ground of the antenna is replaced by an array of patches with different separations from s = 0.1 *mm* to s = 0.9 *mm* between the patches as shown in figure 17. The patch dimensions of 1×0.75 mm^2 offer the best values for an ultra-wide band.

The reflection coefficient of the antenna configuration is shown in figure 17 for ten different separations. It is clear that the separation 0.2 notches the whole band except for the range from 75 GHz to 79 GHz, while the separation 0.3 notches the whole band except for the range from 61 GHz to 79 GHz. However, the separation 0.25 *mm* successfully passes the whole band from 57 GHz to 93 GHz.

For the sake of demonstrating why the ground of the adopted antenna is replaced by an array of patches that

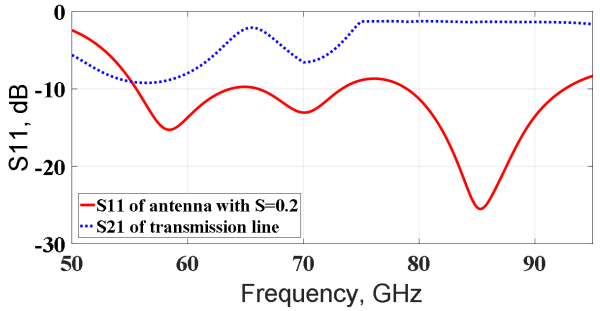

FIGURE 18. Reflection coefficient for separation 0.2 *mm* with transmitted coefficient of S_{21} transmission line with patched ground.

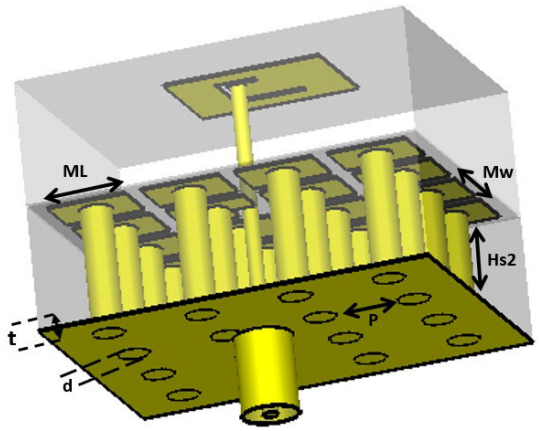

FIGURE 19. Proposed mm-wave antenna using a mushroom ground.

notches some bands and passes others. The wave propagation along a transmission line with patched ground which resembles the meta-material structure is studied. Consider the case of separation of 0.2 *mm*. Figure 18 illustrates the transmission coefficient of the transmission line and also the reflection coefficient of the antenna of the configuration shown in 18 is superimposed. One can notice that the wave propagating along the transmission line is considered as a surface wave preventing the wave from traveling through the antenna structure. Consequently, this leads to decreasing radiation efficiency. In the same time, the structure of the array of patches contributes impedance mismatching with the feed port. These two effects are noticeable in the range from 90 GHz to 95 GHz in figure 18 at which the band is notched.

Concerning the band from 73 GHz to 79 GHz the transmission line passes energy 10% more than the energy intercepted by the antenna. In the same time the patches contribute a fair matching for the antenna structure. The later effect leads to a little notch.

To achieve multi-band, the traditional ground of the antenna is replaced by a mushroom ground as shown in figure 19 where the ground of patches of the antenna is replaced by a grounded mushroom. The grounded mushroom consists of three layers. The first one is the conventional metal sheet ground, the second one is the substrate material Rogers 5880

TABLE 2. Antenna dimensions of the proposed antenna.

Parameter	Value (mm)
hs2	5
Mw	4
ML	0.015
p	0.55
d	0.4

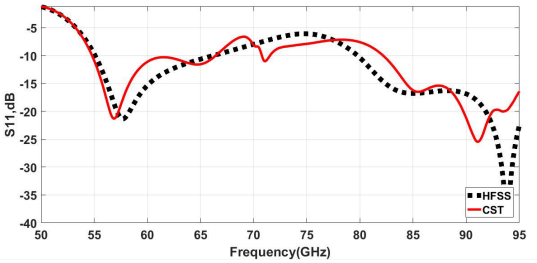

FIGURE 20. Comparison of simulated reflecting coefficient S_{11} using HFSS and CST for mushroom grounded antenna.

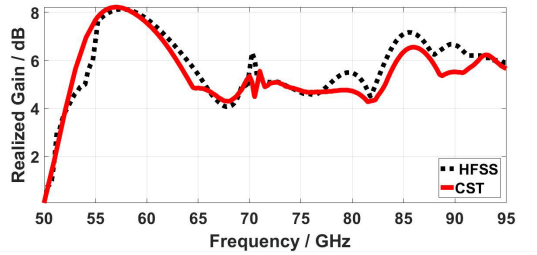

FIGURE 21. Comparison of simulated realized gain using HFSS and CST for mushroom grounded antenna.

of thickness equals to 1.575 *mm*, and the last layer is the array of patches which are connected to the ground using an array of vias. The missing dimensions are presented in table 2.

This structure provides the reflection coefficient illustrated in figure 20 where a multi-band is achieved and operates on the bands from 55 GHz to 68 GHz and 81 GHz to 95 GHz. One notices the good agreement between the results of HFSS and CST. It is very important to point out that the physical reason behind notching the band from 68 GHz to 81 GHz is the propagation of the surface wave along the mushroom grounded transmission line under the antenna structure. It divides the operating band into sub-bands which can be demonstrated by the same methodology previously mentioned for the patched ground antenna.

The realized gain, radiation efficiency and radiation pattern 2D for the mushroom ground base antenna are illustrated in figures 21, 22, and 23 respectively which conducts a good agreement between their simulation results using HFSS and CST. The frequency band, fractional bandwidth, gain, applications and computational methods are depicted in table 3 for the adopted antennas and others in literature. Figures 24 and 25 depict the current distribution along the

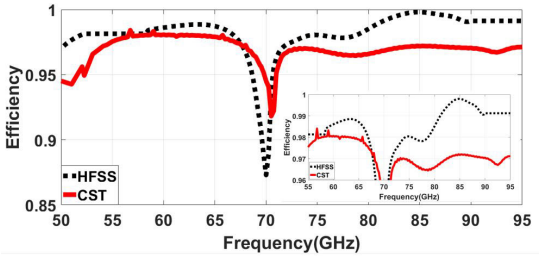

FIGURE 22. Comparison of simulated radiation efficiency using HFSS and CST for mushroom grounded antenna.

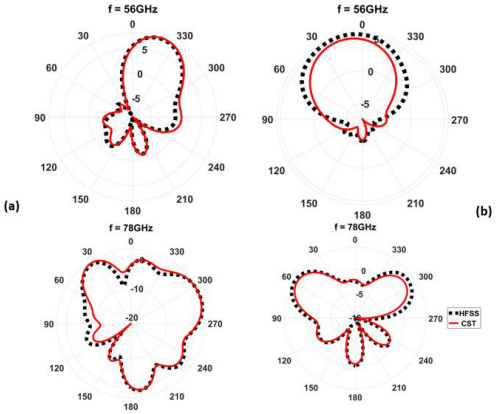

FIGURE 23. Comparison of 2D radiation pattern susing HFSS and CST for mushroom grounded antenna (a) E-plane $\Phi = 0°$ (b) H-plane $\Phi = 90°$.

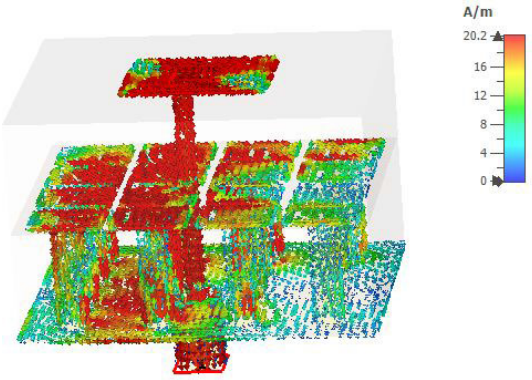

FIGURE 24. Current distribution along the patch and the ground at 57 GHz.

patch and ground layers at the frequencies 57 GHz and 92 GHz respectively. It is noticed that a current is accurately outlined along the antenna edges.

In the microwave band, the antenna covers the bands (5.15-5.825) GHz and (8.025-8.4) GHZ for WiMaX and ITU band applications respectively. In the millimeter band, the antenna covers three bands for Automotive radar applications within (71-76) GHz, (81-86) GHz, and (92-95) GHz [33], [34]. Further 5G applications are planned in the Americas according to the latest ITU release include (24.25-86) GHz band planned for planned for licensed use in

TABLE 3. Comparison between recent papers and this work in millimeter and microwave band.

	Ref	Frequency, Bandwidth, Fractional B.W[GHz%]	Dimensions in λ^2	Applications	Gain (dBi)	Implementation
Microwave band	[7]	(5.35-7), 1.65, 26.7%	1.53x1.23	Differential fed application	7.7-10.7	HFSS, fabrication
	[8]	(7.7-8.5), 0.8, 8.7%	3.78x3.78	MIMO applications	8	Not mentioned and fabricated
	[9]	(5.46-6.27), 0.81, 13.8%	1.66x0.83	Wireless communication systems	7.2-8.9	HFSS, fabrication
	[29]	(5.503-6.12), 0.617, 7.84%	0.9x0.78	Sub 6 GHz	6.89	CST, fabrication
	[30]	(2.4-2.6), 0.4, 56.87%	0.48x0.31	Sub 6 GHz	8	CST, fabrication
	proposed in this paper	(5.5-9.5), 4, 40%	1x1.25	WIMAX, ITU, and 5G applications	5-9	CST, fabrication
mm-wave band	proposed in this paper	(55-95), 40, 40%	1x1.25	5G bands in Canada, Columbia, and USA, Automotive Radar	5-9	CST
	[10]	(58-62), 4, 6.6%	5.08x5.08	Micro-metric mesh metal technology	13.6	CST, fabrication
	[11]	(57-64), 7, 11%	2.22x2.22	16 QAM and MIMO systems	8.6	Not mentioned and fabricated
	[13]	(57-64), 9, 14.2%	1.21x2.96	Unlicensed wide-band application	14.5	Not mentioned and fabricated
	[31]	(53.97-66.06), 6.06, 10%	0.57x0.34	5G and mm-wave	6.54	CST, fabrication
	[32]	(57.57-62.32), 4.75, 8%	1.94x2.66	5G and mm-wave	4.51	CST, fabrication

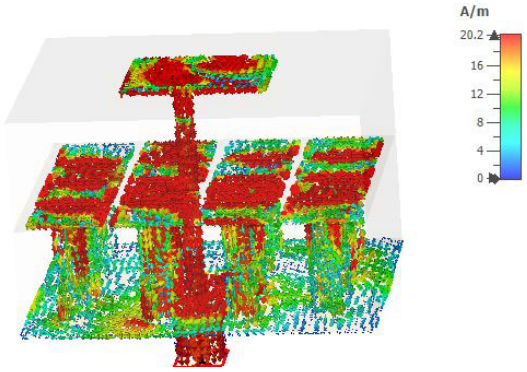

FIGURE 25. Current distribution along the patch and the ground at 92 GHz.

Columbia, (64-71) GHz band planned for shared/unlicensed use in Canada and USA [2], [3], [29]–[32], [35]–[37]. It is clear that the adopted antenna achieves higher fractional bandwidth and can be used in different applications with acceptable gain.

IV. CONCLUSION

The paper presents microwave and mm-wave antennas for UWB and multi-band applications. The microwave antenna achieves a bandwidth of 4.5 GHz (40%) and a average gain of 7dB. It is applied to C-band (4-8) GHz, V-band (40-75) GHz, and W-band (75-110) GHz. The mm-wave antenna covers the bandwidth of 45 GHz (40%) for UWB design and multi-band application for the following bands, the 13 GHz band from 55 GHz to 68 GHz, a 2 GHz band from 70 GHz to 72 GHz and a 13 GHz band from 82 GHz to 95 GHz with gains of 5, 6, and 7dB respectively. It notches the bands (68-70) GHz and (73-83) GHz. It could be used in mm-wave applications for the pass bands.

The antenna is fed using coaxial cable. It is implemented on a Roger 5880 substrate with relative dielectric constant 2.2, thickness 1.575 *mm* and loss tangent 0.0009. To achieve the notches and multi-band applications in mm-wave, the conventional ground is replaced by two different ones. The first one is a ground of an array of patches and the other is a mushroom ground. There is a good matching between the measured and simulated results for the microwave antenna in terms of the reflection coefficient, realized gain, radiation efficiency, and the radiation patterns in the two principle planes. These parameters are in good agreement for the proposed mm-wave antenna that is analyzed using both FEM and FDTD based software.

REFERENCES

[1] C. A. Balanis, *Antenna Theory: Analysis and Design*. Hoboken, NJ, USA: Wiley, 2016.
[2] I. Workshop. (2019). *5G and Spectrum: Different Approaches, iTU Workshop: 5G and New Technologies. Lome, Republic of Togo*. [Online]. Available: https://www.itu.int/en/ITU-D/Regulatory-Market/Documents/Events2019/Togo/5G-Ws/Ses4_Gomes-5Gspectrum-Assignments.pdf
[3] GTW Series. (2019). *IMT in Bands Between 24.25 GHz and 86 GHz to Bolster 5G, WRC Series, WRC-19 Agenda Item 1.13*. [Online]. Available: https://www.gsma.com/spectrum/wp-content/uploads/2019/07/Agenda-Item-1.13-for-5G.pdf
[4] M. Simoni. (2017). *Future Use of Millimetre Waves for 5G, Regional Seminar for Europe and CIS—Spectrum Management and Broadcasting*. [Online]. Available: https://www.itu.int/en/ITU-D/Regional-Presence/Europe/Documents/Events/2017/Spectrum%20Management/Simoni%20-%20Future%20use%20of%20millimetre%20waves%20in%205G%20v1.1.pdf
[5] X. Qu, S. S. Zhong, Y. M. Zhang, and W. Wang, "Design of an S/X dual-band dual-polarised microstrip antenna array for SAR applications," *IET Microw., Antennas Propag.*, vol. 1, no. 2, pp. 513–517, Apr. 2007.
[6] A. Abdelaziz and E. K. I. Hamad, "Design of a compact high gain microstrip patch antenna for tri-band 5G wireless communication," *Frequenz*, vol. 73, nos. 1–2, pp. 45–52, Jan. 2019.
[7] S. Feng, L. Zhang, H.-W. Yu, Y.-X. Zhang, and Y.-C. Jiao, "A single-layer wideband differential-fed microstrip patch antenna with complementary split-ring resonators loaded," *IEEE Access*, vol. 7, pp. 132041–132048, 2019.
[8] P. Mathur and G. Kumar, "Dual-frequency dual-polarised shared-aperture microstrip antenna array with suppressed higher order modes," *IET Microw., Antennas Propag.*, vol. 13, no. 9, pp. 1300–1305, Jul. 2019.
[9] J. Shi, L. Zhu, N.-W. Liu, and W. Wu, "A microstrip Yagi antenna with an enlarged beam tilt angle via a slot-loaded patch reflector and pin-loaded patch directors," *IEEE Antennas Wireless Propag. Lett.*, vol. 18, no. 4, pp. 679–683, Apr. 2019.
[10] A. Martin, O. Lafond, M. Himdi, and X. Castel, "Improvement of 60 GHz transparent patch antenna array performance through specific double-sided micrometric mesh metal technology," *IEEE Access*, vol. 7, pp. 2256–2262, 2019.
[11] T. H. Jang, H. Y. Kim, D. M. Kang, S. H. Kim, and C. S. Park, "60 GHz low-profile, wideband dual-polarized U-slot coupled patch antenna with high isolation," *IEEE Trans. Antennas Propag.*, vol. 67, no. 7, pp. 4453–4462, Jul. 2019.
[12] Z. Chen, Y. P. Zhang, A. Bisognin, D. Titz, F. Ferrero, and C. Luxey, "A 94-GHz dual-polarized microstrip mesh array antenna in LTCC technology," *IEEE Antennas Wireless Propag. Lett.*, vol. 15, pp. 634–637, 2016.
[13] T. H. Jang, H. Y. Kim, I. S. Song, C. J. Lee, J. H. Lee, and C. S. Park, "A wideband aperture efficient 60-GHz series-fed E-shaped patch antenna array with copolarized parasitic patches," *IEEE Trans. Antennas Propag.*, vol. 64, no. 12, pp. 5518–5521, Dec. 2016.
[14] K.-L. Wong and J.-Y. Sze, "Slotted rectangular microstrip antenna for bandwidth enhancement," *IEEE Trans. Antennas Propag.*, vol. 48, no. 8, pp. 1149–1152, Aug. 2000.
[15] E. K. Hamad and G. Nady, "Bandwidth extension of ultra-wideband microstrip antenna using metamaterial double-side planar periodic geometry," *Radioengineering*, vol. 28, no. 1, pp. 25–32, 2019.
[16] J.-H. Lu, "Bandwidth enhancement design of single-layer slotted circular microstrip antennas," *IEEE Trans. Antennas Propag.*, vol. 51, no. 5, pp. 1126–1129, May 2003.
[17] W. Yang and J. Zhou, "Wideband low-profile substrate integrated waveguide cavity-backed E-shaped patch antenna," *IEEE Antennas Wireless Propag. Lett.*, vol. 12, pp. 143–146, 2013.
[18] S.-H. Wi, Y.-S. Lee, and J.-G. Yook, "Wideband microstrip patch antenna with U-shaped parasitic elements," *IEEE Trans. Antennas Propag.*, vol. 55, no. 4, pp. 1196–1199, Apr. 2007.
[19] S. Liao and Q. Xue, "Dual polarized planar aperture antenna on LTCC for 60-GHz antenna-in-package applications," *IEEE Trans. Antennas Propag.*, vol. 65, no. 1, pp. 63–70, Jan. 2017.
[20] Y. Li and K.-M. Luk, "60-GHz dual-polarized two-dimensional switch-beam wideband antenna array of magneto-electric dipoles," in *Proc. IEEE Int. Symp. Antennas Propag. USNC/URSI Nat. Radio Sci. Meeting*, Jul. 2015, pp. 1542–1543.
[21] P. Lee, "Computation of the bit error rate of coherent M-ary PSK with gray code bit mapping," *IEEE Trans. Commun.*, vol. COM-34, no. 5, pp. 488–491, May 1986.
[22] K. D. Xu, H. Xu, Y. Liu, J. Li, and Q. H. Liu, "Microstrip patch antennas with multiple parasitic patches and shorting vias for bandwidth enhancement," *IEEE Access*, vol. 6, pp. 11624–11633, 2018.
[23] W. Liu, Z. N. Chen, and X. Qing, "60-GHz thin broadband high-gain LTCC metamaterial-mushroom antenna array," *IEEE Trans. Antennas Propag.*, vol. 62, no. 9, pp. 4592–4601, Sep. 2014.
[24] Y. Shi, W. Feng, X. Jiang, Q. Xue, and W. Che, "Half-air-filled ball-grid-array-based substrate-integrated groove-gap waveguide and its transition to microstrip at W-band," *IEEE Trans. Microw. Theory Techn.*, vol. 68, no. 12, pp. 5145–5153, Dec. 2020.

[25] K. Issa, H. Fathallah, S. Alshebeili, M. A. Ashraf, and H. Vettikalladi, "Broadband high-gain antenna for millimetre-wave 60-GHz band," *Electronics*, vol. 8, no. 11, p. 1246, Oct. 2019, doi: 10.3390/electronics8111246.
[26] J. Li, J. Shi, L. Li, T. A. Khan, J. Chen, Y. Li, and A. Zhang, "Dual-band annular slot antenna loaded by reactive components for dual-sense circular polarization with flexible frequency ratio," *IEEE Access*, vol. 6, pp. 64063–64070, 2018.
[27] Y. Al-Alem and A. A. Kishk, "High-gain 60 GHz slot antenna with symmetric radiation characteristics," *IEEE Trans. Antennas Propag.*, vol. 67, no. 5, pp. 2971–2982, May 2019.
[28] Y. Al-Alem and A. A. Kishk, "Wideband millimeter-wave dielectric resonator antenna with gain enhancement," *IEEE Antennas Wireless Propag. Lett.*, vol. 18, no. 12, pp. 2711–2715, Dec. 2019.
[29] K. N. Olan-Nunez, R. S. Murphy-Arteaga, and E. Colin-Beltran, "Miniature patch and slot microstrip arrays for IoT and ISM band applications," *IEEE Access*, vol. 8, pp. 102846–102854, 2020.
[30] B. Huang, M. Li, W. Lin, J. Zhang, G. Zhang, and F. Wu, "A compact slotted patch hybrid-mode antenna for sub-6 GHz communication," *Int. J. Antennas Propag.*, vol. 2020, pp. 1–8, Jul. 2020.
[31] R. Arora, S. B. Rana, and S. Arya, "Performance analysis of Wi-Fi shaped SIW antennas," *AEU-Int. J. Electron. Commun.*, vol. 94, pp. 168–178, Sep. 2018. [Online]. Available: http://www.sciencedirect.com/science/article/pii/S1434841118304333
[32] T. Okan, "Design and analysis of a quad-band substrate-integrated-waveguide cavity backed slot antenna for 5G applications," *Int. J. RF Microw. Comput.-Aided Eng.*, vol. 30, no. 7, Jul. 2020, Art. no. e22236. [Online]. Available: https://onlinelibrary.wiley.com/doi/abs/10.1002/mmce.22236
[33] A. Tamayo-Dominguez, J.-M. Fernandez-Gonzalez, and M. Sierra-Castaner, "3-D-printed modified butler matrix based on gap waveguide at W-band for monopulse radar," *IEEE Trans. Microw. Theory Techn.*, vol. 68, no. 3, pp. 926–938, Mar. 2020.
[34] W. Wei and X. Wang, "A 77 GHz series fed weighted antenna arrays with suppressed sidelobes in E- and H-plane," *Prog. Electromagn. Res. Lett.*, vol. 72, pp. 23–28, 2018.
[35] N. K. Mungaru and T. Shanmuganantham, "Substrate-integrated waveguide-based slot antenna for 60 GHz wireless applications," *Microw. Opt. Technol. Lett.*, vol. 61, no. 8, pp. 1945–1951, Aug. 2019. [Online]. Available: https://onlinelibrary.wiley.com/doi/abs/10.1002/mop.31841
[36] N.-W. Liu, L. Zhu, W.-W. Choi, and J.-D. Zhang, "A low-profile differentially fed microstrip patch antenna with broad impedance bandwidth under triple-mode resonance," *IEEE Antennas Wireless Propag. Lett.*, vol. 17, no. 8, pp. 1478–1482, Aug. 2018.
[37] N.-W. Liu, L. Zhu, W.-W. Choi, and X. Zhang, "A low-profile aperture-coupled microstrip antenna with enhanced bandwidth under dual resonance," *IEEE Trans. Antennas Propag.*, vol. 65, no. 3, pp. 1055–1062, Mar. 2017.

SARA YEHIA ABDEL FATAH was born in Cairo. She received the M.Sc. degree from the Arab Academy for Science and Technology, in 2014. She is currently pursuing the Ph.D. degree with Aswan University. She has worked as an Assistant Lecturer with the Egyptian Chinese University in Cairo for eight years.

EHAB K. I. HAMAD received the B.Sc. and M.Sc. degrees in electrical engineering from Assiut University, Egypt, in 1994 and 1999, respectively, and the Ph.D. degree in electrical engineering from the University of Magdeburg, Germany, in 2006. From 1996 to 2001, he was a Teaching/Research Assistant with the Aswan Faculty of Engineering, South Valley University. From July 2001 to December 2006, he was a Research Assistant in the Chair of Microwave and Communication Engineering, Otto-von-Guericke University Magdeburg, Magdeburg, Germany. From July 2010 to April 2011, he joined the School of Computing and Engineering, University of Huddersfield, Huddersfield, U.K., as a Postdoctoral Research Assistant. He is currently a Full Professor for Antennas Engineering at the Department of Electrical Engineering, Faculty of Engineering, Aswan University, Aswan, Egypt. He has authored and coauthored over 47 technical peer-reviewed papers in international journals and conference proceedings and received one best paper award. His current research interests include antenna design, Microstrip antennas, MIMO antennas, mm-wave antennas, multi-band/wide-band small antennas for 4G/5G, metamaterials, metasurfaces, UWB, RFID, and RF energy harvesting. He is currently working on designing microstrip antennas for 5G wireless communications using characteristics mode analysis. He is a reviewer of many journals, including the IEEE TRANSACTIONS ON ANTENNAS AND PROPAGATION, *IET Microwaves, Antennas, and Propagations*, *Electronics Letters*, *Radio engineering*, *PIERs*, *The Journal of Electrical Engineering*, the *Journal of Recent Advances in Electrical & Electronic Engineering*, and *Optical Microwave Technology Letters* as well as many international conferences, including EuCAP, National Radio Sciences, and Asia-Pacific Microwave Conference and some others on EasyChair and EDAS.

WAEL SWELAM was born in Egypt, in 1971. He received the B.Sc. degree in electrical engineering with the Communications Department, Military Technical College (MTC), Cairo, Egypt, with the graduation grade of "Excellent", cumulative grade of "Very Good with Honor", and GPA = 3.5 (30th June 1993), the M.Sc. degree in electrical engineering technology with the Benha Faculty of Engineering, Benha University, Benha, Egypt, with a thesis title of "Computer Aided Design of Surface Acoustic Wave Filters for Mobile Communications," 8th November 2001, and the Ph.D. degree in electrical engineering from the Military Technical College (MTC), Cairo, Egypt, with a thesis title of "Design and Realization of a Microwave Planar Active Antenna Array," 5th September 2006. His current area of researches include nano antennas and microwave circuits, 3G, 4G & 5G wireless mobile antenna systems, MIMO antenna systems, satellite antenna systems, active phased array antennas, millimetric & sub-millimetric antenna systems, microstrip antenna systems & microwave circuits, vehicles automation, and navigation systems.

A. M. M. A. ALLAM was born in Cairo, Egypt, in 1955. He received the B.S. and M.S. degrees in electrical engineering from MTC and Cairo University, in 1978 and 1985, respectively, and the Ph.D. degree in electrical engineering from Kent University, U.K., in 1988. From 1978 to 1980, he was an Engineer in Airforce in Egyptian Army, working for maintenance and repair for airborne equipment in C-130 aircraft, where he was a crew member in that interval. From 1981 to 1984, he was a Researcher and Instructor in the air born equipment's Department, MTC, Cairo, Egypt, where he has been a Lecturer and Researcher, since 1988. He was granted Associate Professorship and Professorship, in 1995 and 2000, respectively. He was the Dean and Deputy Commandant of the MTC, Cairo, Egypt. He was also the Dean and Vice Dean of the Faculty of Information Engineering & Technology, German University in Cairo, Egypt, where he is currently the Head of the Communication Department. He has published hundreds of conference and journal papers. He did a lot of applied research in RADAR absorbing materials. His research interests lie in RF and microwave technology, antenna design, smart antennas for vehicles and radar sensors, satellite communication, and diagnoses of censer based on the electromagnetic properties of human organisms.

MOHAMED FATHY ABO SREE was born in Egypt. He received the M.Sc. degree from the Arab Academy for Science and Technology (AASTMT), in 2013, and the Ph.D. degree in electrical engineering from Ain Shams University, Egypt, in 2019. His research interests include antenna design and MW technology. He is reviewing in IEEE Access and *PIER on-line Journal*.

HESHAM A. MOHAMED (Member, IEEE) received the B.Sc. degree in electronics and communication engineering from the University of Menofia, in 2003, and the M.Sc. and Ph.D. degrees from Ain Shams University, in 2009 and 2014, respectively. He is currently a Researcher with the Electronics Research Institute (ERI), Giza, Egypt. He has Teaching Experience (more than 12 years' experience) as a Lecturer with the Electronic and Communication Engineering Department, Faculty of Engineering, Misr University for Science and Technology. He has authored or coauthored close to 20 journal papers and about 17 refereed conference papers, as well as attended and chaired several national and international conferences. He has supervised and co-supervised two Ph.D. and two M.Sc. theses at the Cairo University, Ain shams University, and Helwan University, the outstanding publications of my work in ranked international journals and conferences. His research interests are on microwave circuit designs, planar antenna systems, recently on EBG structures, UWB components and antenna and RFID systems, radar absorbing materials, energy harvesting and wireless power transfer, smart antennas, microstrip antennas, microwave filters, metamaterials, as well as MIMO antennas and its applications in wireless communications. He is a reviewer at the International Journals, i.e., IEEE Microwave and Wireless Components Letters, IEEE Access, *Progress in Electromagnetics Research* (PIER, PIER B, C, M, PIER Letters), *Microwave and Optical Technology Letters*, and *International Journal of Circuit Theory and Applications*. He participates in more than six research projects at the national and international levels as Egypt- NSF-USA Joint Fund Program, Egypt STDF-France IRD Joint Fund Program, and the European Committee programs of FP6 and FP7. His role is from C-PI to PI. As RF-Design Engineer (Antenna and Power Amplifier Module) (2018–2020) in the project ''Small SAR satellite antenna and transceiver system'' and Communication Subsystem Engineering (2019–2020) in the project ''Egyptian University Satellite (EUS-2)'' RF-Design Engineer (2018-2019) in the project ''Design of Radar Absorbing Materials (RAM) using Meta-materials'' Wireless System Engineering, in the project (2015-2018) ''Development of High Data Rate X-Band Transmitter for LEO Remote Sensing Satellites'' RF-Design Engineer (2015-2018) in the project ''THE EGYPTION 2D RADAR'' RF-Design Engineer (2011-2014) in the project ''Ultra-wideband Ground Penetrating Radar for Water Detection in Egypt'' and RF-Design Engineer (2011-2014) Feb. 2011- Feb. 2014 ''Novel Planar Antennas for the Most Recent Telecommunications Applications.''